metals

MDPI

Article

Optimization of Electrical Conductivity and Hardness in Al-1Si Alloy Through Mg/Fe Alloying and Heat Treatment

Xiaoli Cui [1,2,*], Houyun Liu [2], Yan Wang [2], Chao Lu [1], Wenqing Shi [1] and Di Tie [1]

[1] School of Materials Science and Engineering, Guangdong Ocean University, Yangjiang 529500, China
[2] School of Materials Science and Engineering, Shandong University of Technology, Zibo 255000, China
* Correspondence: cuixiaoli111@163.com; Tel.: +86-13011623676; Fax: +86-0662-2162085

Abstract: In this study, a new kind of the Al-1Si-0.6Mg-0.2Fe alloy was fabricated by Mg, Fe alloying treatment and the influence mechanism of Mg, Fe on electrical conductivity (EC) and Vickers hardness (HV) of the Al-1Si alloy was analyzed by the combination of experiments and simulations. Results showed that during the solidification process, intermediate phase $Al_8FeMg_3Si_6$ formed which can inhibit the growth of needle-like AlFeSi phase, resulting in a more refined distribution of AlFeSi particles and this is helpful to improve EC and HV simultaneously. According to the simulation results, Al-1Si-0.6Mg-0.2Fe generated the most $Al_8FeMg_3Si_6$ and the corresponding EC and HV reached 48.5% IACS and 62.9 HV, respectively. Furthermore, during heat treatment process, AlFeSi can promote the nucleation of Mg_2Si, reducing the elemental solution of Mg and Si. With 550 °C/2 h + 210 °C/24 h heat treatment, on the one hand, oversized needle-shaped AlFeSi fused to smaller particles and distributed more uniformly. On the other hand, more solid solution Si and Mg precipitated with form of Mg_2Si. Finally, the EC and HV of Al-1Si-0.6Mg-0.2Fe improved to 54.5% IACS and 79.8 HV, achieving the simultaneous optimization of EC and HV. This can provide theoretical guidance for the preparation of high strength and high conductivity aluminum alloy.

Keywords: Al-1Si-0.6Mg-0.2Fe alloy; alloying treatment; heat treatment; electrical conductivity (EC); vickers hardness (HV)

check for updates

Academic Editor: Koh-ichi Sugimoto

Received: 24 December 2024
Revised: 18 February 2025
Accepted: 28 February 2025
Published: 14 March 2025

Citation: Cui, X.; Liu, H.; Wang, Y.; Lu, C.; Shi, W.; Tie, D. Optimization of Electrical Conductivity and Hardness in Al-1Si Alloy Through Mg/Fe Alloying and Heat Treatment. *Metals* **2025**, *15*, 317. https://doi.org/10.3390/met15030317

Copyright: © 2025 by the authors. Licensee MDPI, Basel, Switzerland. This article is an open access article distributed under the terms and conditions of the Creative Commons Attribution (CC BY) license (https://creativecommons.org/licenses/by/4.0/).

1. Introduction

Due to low density and the relatively high intrinsic conductivity of aluminum, aluminum based composites or alloys are chosen as the best candidates for Cu conductive materials [1–3]. With the continuous development of electrically conductive industry, higher demands for improving mechanical properties without sacrificing the electrical conductivity (EC) are proposed [1,4–7]. Generally, primary methods to improve mechanical properties are solid solution strengthening, second-phase strengthening, deformation strengthening, and fine-grain strengthening. However, according to Matthiessen's rule [4,8], either the lattice distortion, second-phase particles produced by alloying, or the increase in dislocation density due to deformation strengthening can improve the mechanical properties but damage the electrical conductivity. Nevertheless, sacrificing EC or mechanical properties will significantly limit the application of aluminum conductive materials. But if we can modify the influence factors, such as amount of alloying elements, grain boundary, lattice distortion, existence statement of second-phase particles, etc., it is possible to achieve good matching relationship between EC and mechanical properties of aluminum conductive alloys. Improving mechanical properties by alloying treatment is currently a hot

research topic [9,10]. However, the presence forms of alloying elements is important. The damage of alloying elements with solid solution statement to EC is much greater than that of an equal concentration with precipitation state, and it is often by one or two orders of magnitude. The underlying reason is that alloying elements with solid solution statement can induce obvious lattice distortions which increasing more scattering of free electrons during transport than that with precipitation state [11]. Chen et al. studied the effects of Er additions on the microstructure, mechanical properties and electrical conductivity of the Al-0.4Fe-0.05Si alloy, and with 0.2% Er addition, the electrical conductivity of the rolled Al-0.4Fe-0.05Si-0.2Er alloy increased from 60.1 to 62.2% IACS, and the hardness decreased from 50.5 to 36.6 HV [2]. KARABAY S et al. fabricated a kind of the AA6201 alloy with extra high conductivity, property of high tensile stress by artificial aging heat treatment [5]. Liang et al. reported that the tensile strength and thermal-resistant property of the Al-Mg-Si alloy are improved by Zr addition [10]. So, for alloying treatment, it is important to control the statement of alloying elements and in order to achieve a good electrical conductivity, it prefers to promote more alloying elements existed with form of second phase precipitation.

Among aluminum conductive materials, hypoeutectic Al-Si alloys are widely used in overhead transmission lines or other fields due to their low price, good electrical and thermal conductivity, and high mechanical properties. But during aluminum melt treatment process, most of the melting appliances used are made of steel, and Fe is an unavoidable alloying element for aluminum alloy, which usually contains 0.1–0.3% and it is challenging to remove Fe from industrial Al [12]. Zhao et al. proposed a method that adding Fe to the Al-Si alloy and forming AlFeSi phase to reduce the damage of solution Si to EC [6], so for aluminum conductive materials, the damage of Fe or Si alloying element to EC can be reduced by forming AlFeSi precipitated phase. In addition, Mg is an important alloying element and adding appropriate amounts of Mg to the Al-Si alloy can further improve the mechanical property of the Al-Si alloy by forming nanoscale Mg_2Si particles after heat treatment. So, proper Mg and Fe alloying elements should be added to the hypoeutectic Al-Si alloy to fabricate aluminum conductive materials with high electrical conductivity and mechanical property [13–16].

In this study, we choose Al-1Si alloy as the main research alloy, and the effect of Mg, Fe on EC and HV of the Al-1Si alloy was investigated by a combination of experiments and simulations. Firstly, adding trace Mg and Fe to the Al-Si alloy to form AlFeSi and Mg_2Si phases, and the solid solution Si content in the Al-Si alloy can be reduced, and a suitable combination of Fe/Si ratio and Mg/Si ratio was found to achieve the effect of "controlling Si by Mg and Fe". As calculations based on theoretical phase diagram, JMatPro 10.0 simulation software helps us analyze the relationship between alloying element type, content and temperature during solidification process [17–23]. And this is applicable to multiple systems, such as general-purpose steels [18], nickel alloys [19], aluminum alloys, etc. [20–23]. In order to better illustrate the influence mechanism of Mg, Fe addition on microstructure and properties, this study simulates the solidification process of Al-1Si-xFe-yMg (x = 0.1, 0.2, 0.3; y = 0.3, 0.6, 0.9, 1.2) by using JMatPro software. Thirdly, a simple solution-aging heat treatment was carried out and control the amount and size of precipitates to further optimize the matching of EC and HV. Finally, through analyzing the influence of Mg, Fe alloying treatment and heat treatment on EC and HV, a kind of Al-1Si-0.6Mg-0.2Fe alloy with good matching between EC and HV was fabricated successfully, which has a promising application in the field of electrical engineering. This study can provide theoretical guidance for developing high EC and high-strength conductive Al-Si alloys. The promotion and application of aluminum and aluminum alloy materials in the fields of large-span transmission lines and power fittings and equipments. It helps to achieve high-efficiency, energy-saving, environmental protection and lightweight of

large-span transmission lines, which is of great strategic significance for the sustainable development of our country, efficient energy utilization, and accelerating the realization of the "double carbon" task goal.

2. Experimental Process

2.1. Sample Preparation

This study used industrial aluminum of 99.7%, pure Si of 99.5%, Fe of 99.9%, and pure Mg of 99.9% as raw materials. Firstly, 99.7% industrial aluminum was melted in a resistance furnace at 750 ± 10 °C. The aluminum melt was de-slagged and degassed using 0.5% C_2Cl_6 and stirred for 2 min. Then, pure Si was added to the aluminum melt and poured into a steel mold preheated at 220 ± 5 °C to prepare the Al-1Si alloy ingots. To investigate the effect of Fe element on EC and HV of Al-1Si alloy, after melting the Al-1Si alloy at 750 ± 10 °C in a resistance furnace, different contents of Fe (0.1 wt.%, 0.2 wt.%, 0.3 wt.%) (wt.% is abbreviated as %) elements were added. After choosing the best Fe addition, different Mg contents (0.3%, 0.6%, 0.9%, 1.2%) were added to the alloy. As the density of Mg is much less than aluminum, we use apparatus to press the Mg wrapped by aluminum foil to the bottom of aluminum melt, and after 2–3 min, stirred it thoroughly. Finally, we poured the aluminum melt into a metal mold to obtain a standard EC test bar (Φ16.5 mm × 140 mm). Other melting processes were the same as for the alloys mentioned above. After determining the best alloy composition, a simple solution-aging heat treatment was carried out for the test bars (550 °C/2 h + 210 °C/ (0.5 h, 1 h, 3 h, 5 h, 8 h, 16 h, 24 h, 36 h, 72 h). The main experimental procedure is shown in Figure 1.

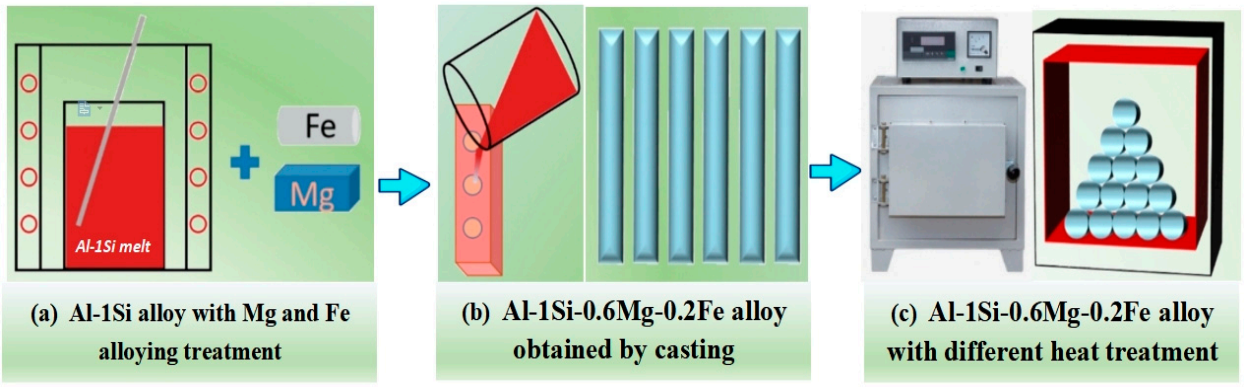


Figure 1. The main experimental flow of this study.

2.2. Performance and Microstructure Analysis

The electrical conductivity properties test bars were machined to rod type specimens (10 mm in diameter and 150 mm in length) and examined by a four pole method XH1000 high precision resistivity tester RS.03-DX200 (Xi'an Honghu Testing Instrument Co., Ltd., Xi'an, China). The unit of electrical conductivity is %IACS (International Annealed Copper Standard). The tester was calibrated by Fluke8845A (An'Tai technology Co., Ltd., Xi'an, China) and BZ3 direct current standard resistance. The EC can be calculated by the following Equation (1) [4].

$$EC = \frac{4 \times L_{rob}}{\pi \times d^2 \times R \times 5.8 \times 10^7} \times 100\% \quad (1)$$

where L_{rod} is the length of the test conductive rod (unit: mm); d is the average diameter of the test conductive rod pair (unit: mm); and R is the resistance of the test conductive rod. Furthermore, the samples are tested for hardness using a micro-vickers hardness tester

with a test load of 200 g and a holding time of 15 s. Seven points are measured for each sample and averaged.

The specimens of chemical composition and microstructure analysis needed to be polished with different particle sizes (360#, 800#, 1000# and 1200#) of SiC sandpapers, finally polished with the polishing cloth on a polishing machine. The chemical compositions of the alloys in this work were confirmed by spectral analysis and the spectral analysis was performed by a SPECTRO MAXx Spectral analyzer (Ametek Group-Speck Analytical Instruments GMBH, Berlin, Germany) (the detection accuracy is ~ppm). Metallographic samples were mechanically grounded and polished through standard routines. The microstructure analysis was carried out by field emission scanning electron microscopy (FESEM). FESEM investigations were carried using a SU-70 scanning electron microscope (Hitachi Production Co., Ltd., Tokyo, Japan) operated at 15 keV and linked with an energy dispersive X-ray spectroscopy (EDX) attachment. Furthermore, an X-ray diffractometer (abbreviated to XRD, Bruker AXS D8 Advance (Bruker Instruments Co., Ltd., Berlin, Germany)) is employed for phase identification. All tests and analysis were performed at room temperature.

3. Results and Discussion

3.1. Effect of Mg and Fe Alloying on EC and HV of Al-1Si Alloy

Figure 2 shows the effect of alloying treatments with different Mg, Fe contents on the EC and HV of Al-1Si alloy. With Fe/Mg content increasing, the matching EC and HV degrees of the Al-1Si alloy change significantly. From Figure 2a, when Fe addition reaches 0.1%, 0.2%, and 0.3%, the EC decrease rates are 3.7%, 5.5%, and 7.7%, and the HV growth rates are 10.1%, 20.6%, and 28.2%, respectively. By analyzing it can be found that the EC decrease and the HV increase are almost linear with the increase in Fe or Mg contents. In this work, a concept of "exchange rate" is proposed, which is the ratio of HV growth rate to EC decrease rate and the higher the exchange rate, the better trade-off between EC and HV of the alloy. It is used to illustrate the match relationship between EC and HV. From Figure 2c, the exchange rate of Al-1Si-0.2Fe alloy is the highest, which is 3.7. Thus, Al-1Si-0.2Fe is considered to be the best match between EC and HV. Then, the effect of Mg on EC and HV of the Al-1Si-0.2Fe alloy is studied and the changes in exchange rate is analyzed. Identically, the Al-1Si-0.6Mg-0.2Fe alloy has the highest exchange rate of 5.7 and is considered to be the best match between EC and HV, as shown in Figure 2d.

To better illustrate the influence of alloying elements on alloys' properties, physical phase composition and microstructure of the alloys are investigated. Figure 3 shows the microstructure of Al-1Si-0.2Fe and Al-1Si-0.6Mg-0.2Fe alloys. From Figure 3a,c, it is found that AlFeSi particles distributed along the grain boundaries with form of large-size pin-striped second phase. And Al-1Si-0.2Fe appears to have highly interconnected networks of intermetallic phases which can easily cleave aluminum matrix and significantly increase electron scattering, so this can damage EC and HV. From Figure 3b, it is found that adding Mg to the Al-1Si-0.2Fe alloy resulted in formation of more small-sized second phases. It consumes more Si which can reduce the amount of Si solution and changes the morphology of eutectic Si which breaks the network phenomenon and facilitates the electrons transmission, as shown in Figure 3d. In order to better illustrate the influence mechanism of Mg and Fe addition on microstructure and comprehensive properties, this study simulates the solidification process of Al-1Si-xFe-yMg (x = 0.1, 0.2, 0.3; y = 0.3, 0.6, 0.9, 1.2) by using JMatPro software.

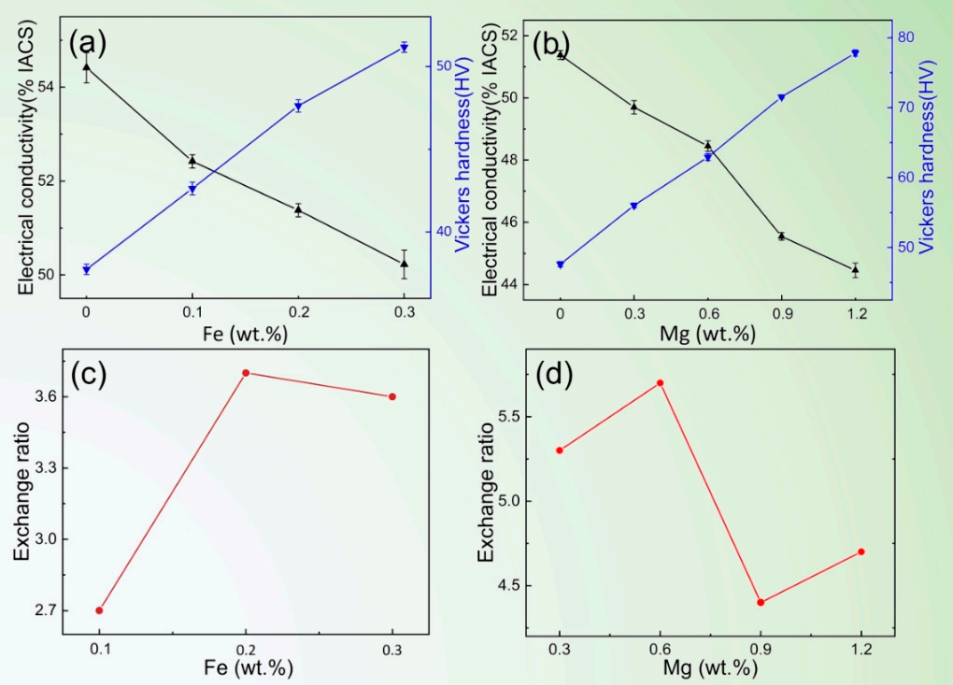


Figure 2. (**a**) EC and HV of Al-1Si-xFe; (**b**) EC and HV of Al-1Si-0.2Fe-yMg; (**c**) exchange rate of Al-1Si-xFe; (**d**) exchange rate of Al-1Si-0.2Fe-yMg (for x = (0), 0.1, 0.2, and 0.3, and y = (0), 0.3, 0.6, 0.9, and 1.2).

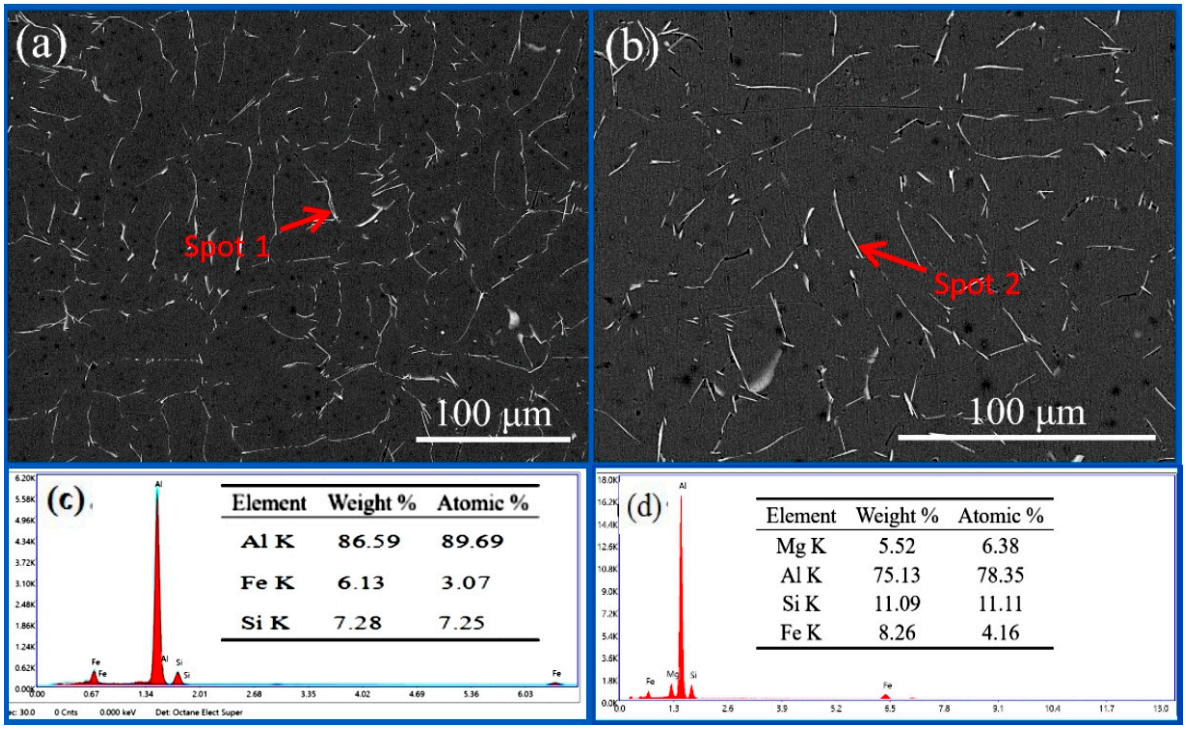


Figure 3. Microstructure photographs of cast alloys: (**a**) Al-1Si-0.2Fe; (**b**) for Al-1Si-0.6Mg-0.2Fe; (**c**) and (**d**) are EDX analysis at point 1 and point 2, respectively.

Figure 4 shows JMatPro simulation results of Al-1Si based alloys. From Figure 4a–k, during solidification process, the percentage of β-AlFeSi phase keeps the same with the increasing of Mg at the constant Fe content but owing to the influence of Mg addition, part of Si phase transforms to Mg_2Si phase. It is also noted that during the solidification,

owing to the addition of Mg, Fe addition, intermediate phase $Al_8FeMg_3Si_6$ forms and then decomposes into β-AlFeSi phase, Mg_2Si phase, and Si at 397.7 °C, which provides more possibility for improving of mechanical properties with heat treatment. Thus, we speculate that during the solidification of Mg-containing Al-1Si-0.2Fe, the AlFeSi growth is inhibited due to the formation of $Al_8FeMg_3Si_6$ phase, which snatches Fe. Therefore, the alloy allows maximum inhibition of AlFeSi growth and allows forming more Mg_2Si, resulting in the highest matching of EC and HV. More small-sized AlFeSi and Mg_2Si phases appear, reducing the effect of second phase on electron scattering and increasing the second phase strengthening. As shown in Figure 4f (marked with red star), during the solidification process of Al-1Si-0.6Mg-0.2Fe alloy, the content of $Al_8FeMg_3Si_6$ phase is the highest and in this condition, it can promote more solution Si precipitate with form of Mg_2Si and we can control the size and statement of Mg_2Si to make it maintain a good lattice match with the aluminum matrix. At the same time, as shown in Table 1, the Al-1Si-0.6Mg-0.2Fe alloy forms the largest mass percent of $Al_8FeMg_3Si_6$ phase during solidification with a mass percent of 1.83%. As intermediate phase $Al_8FeMg_3Si_6$ is effectively captured Fe atoms and inhibited the growth of needle-like AlFeSi structures, resulting in a more refined distribution of AlFeSi particles, which is helpful to improve both EC and HV. The simulation results are in agreement with the experimental results, as shown in Figure 2d. So, the Al-1Si-0.6Mg-0.2Fe alloy is chosen as the optimum alloy composition. For the Al-1Si-0.6Mg-0.2Fe alloy, its properties can be strengthened by heat treatment, so to further optimize the matching of EC and HV, T6 heat treatment is proceeded.

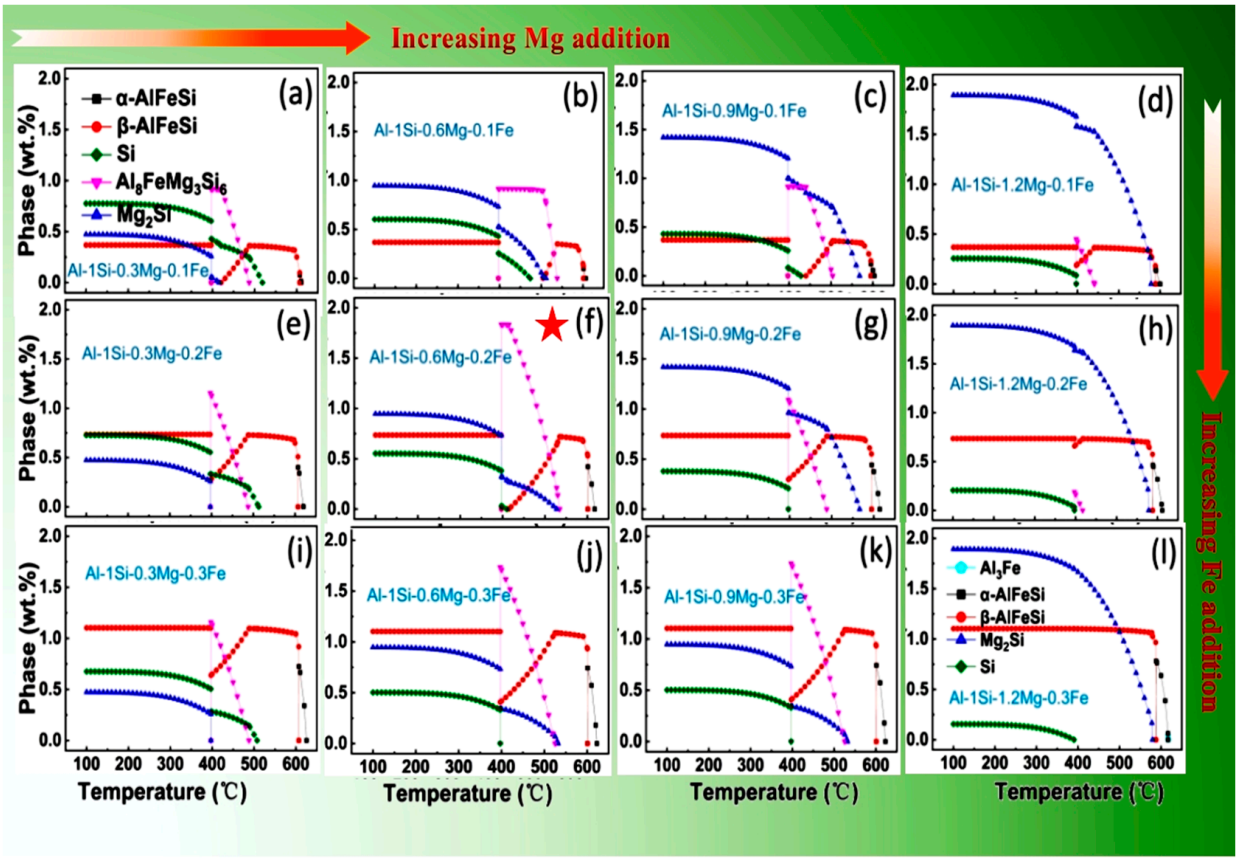


Figure 4. JMatPro simulation analysis about the influence of Mg and Fe addition on Al-1Si based alloys: (**a**–**l**) are corresponding to Al-1Si-xFe-yMg (x = 0.1, 0.2, 0.3; y = 0.3, 0.6, 0.9, 1.2) alloys with different temperatures.

Table 1. JMatPro software simulation: second phase and intermediate products produced by the alloy during condensation (unit: wt.%).

Alloy Composition (wt.%)	Second Phase (wt.%)			Intermediate Products (wt.%)		
	Si	Mg_2Si	β-AlFeSi	α-AlFeSi	$Al_8FeMg_3Si_6$	Al_3Fe
Al-1Si-.3Mg-0.1Fe	0.78	0.47	0.37	0.08	0.92	\
Al-1Si-0.6Mg-0.1Fe	0.60	0.95	0.37	0.10	0.92	\
Al-1Si-0.9Mg-0.1Fe	0.43	1.42	0.37	0.12	0.92	\
Al-1Si-1.2 Mg-0.1Fe	0.26	1.89	0.37	0.15	0.45	\
Al-1Si-0.3Mg-0.2Fe	0.73	0.47	0.74	0.40	1.15	\
Al-1Si-0.6Mg-0.2Fe	***0.55***	***0.95***	***0.74***	***0.42***	***1.83***	\
Al-1Si-0.9Mg-0.2Fe	0.38	1.42	0.74	0.44	1.09	\
Al-1Si-1.2 Mg-0.2Fe	0.21	1.89	0.74	0.46	0.19	\
Al-1Si-0.3Mg-0.3Fe	0.68	0.47	1.10	0.73	1.16	\
Al-1Si-0.6Mg-0.3Fe	0.50	0.95	1.10	0.74	1.73	\
Al-1Si-0.9Mg-0.3Fe	0.33	1.42	1.10	0.76	0.83	\
Al-1Si-1.2 Mg-0.3Fe	0.15	1.89	1.10	0.78	\	0.04

3.2. Effect of Heat Treatment on EC and HV of Al-1Si-0.6Mg-0.2Fe Alloy

It is well known that the properties of alloys are influenced by the existential state of alloying elements. As the solid solution of atoms in aluminum alloy influences EC to a much greater extent than an equal concentration of the second phase. This study wants to optimize the matching relationship between EC and HV by making the solid solution atoms precipitate through heat treatment process, forming a large number of second phases. Figure 5 shows the effect of heat treatment on EC and HV of Al-1Si-0.6Mg-0.2Fe alloy. With the aging time increasing, EC of the alloy increased exponentially followed by a linear increase. When the aging time reaches 24 h, the EC reaches 54.5% IACS, which is 11.7% higher than the Al-1Si-0.6Mg-0.2Fe alloy as-cast (48.8% IACS). By analyzing Figure 5b, HV of the alloy showed a phenomenon of firstly increasing and then decreasing. By analyzing, it is easy to found that with the increasing aging time, EC of Al-1Si-0.6Mg-0.2Fe alloy continues to increase and this is because that during aging process, more alloying elements precipitate and the corresponding aluminum matrix lattice distortion becomes smaller, which is helpful to the efficient electron transmission. While, combined with the change in HV, when aging time is 8 h, it reaches peak aging hardness and with the increasing aging time, HV decreases gradually. So, considering the optimal trade-off between EC and HV, aging time 24 h is optimal. When the aging time reached 24 h, the HV was 79.8 HV, which is 26.9% higher compared to the Al-1Si-0.6Mg-0.2Fe alloy as-cast (62.9 HV).

To investigate the influence mechanism of heat treatment on properties, the effect of T6 heat treatment on microscopic composition and microstructure is researched. Figure 6 is XRD analysis of Al-1Si-0.6Mg-0.2Fe before and after heat treatment (the heat-treated diffractograms shifted vertically). It can be seen that the diffraction peaks indicate the presence of Al, Si, AlFeSi, Mg_2Si, AlMg, Al_6Fe, and $Al_8FeMg_3Si_6$ phases. After heat treatment, more Mg_2Si appears. In addition, the five peaks at 38.5°, 44.7°, 65.1°, 78.2°, and 82.4° are corresponding to Al phase, respectively. Furthermore, as a result of T6 heat treatment, static recrystallization occurs, resulting in a larger grain size, and the peaks become narrower. Additionally, it is worth mentioning that the diffraction peaks of α-Al shift toward to higher 2θ, which implies the precipitation of solid solution elements from aluminum matrix and forming more second phases. To further analyze the interfacial relationship between AlFeSi and Mg_2Si particles, the edge-to-edge matching (E2EM) model proposed [24] is used to evaluate the crystal mismatch between the two phases. In general, with more than four pairs of low crystal plane index crystallographic surface mismatch of less than 6%, it is considered that the two-phase interface is well matched and easy to

heterogeneous nucleation [25]. In addition, it is in agreement with the results of the JMatPro software simulation of that AlFeSi is formed before Mg_2Si during solidification. Thus, from the calculation results in Table 2, the AlFeSi has a good lattice-matching relationship with Mg_2Si. So AlFeSi can provide a heterogeneous-shaped nucleation site for Mg_2Si, promoting more Mg_2Si forming and reducing the content of Si solution to some extent. This is helpful to improve the EC of Al-1Si-0.6Mg-0.2Fe alloy.

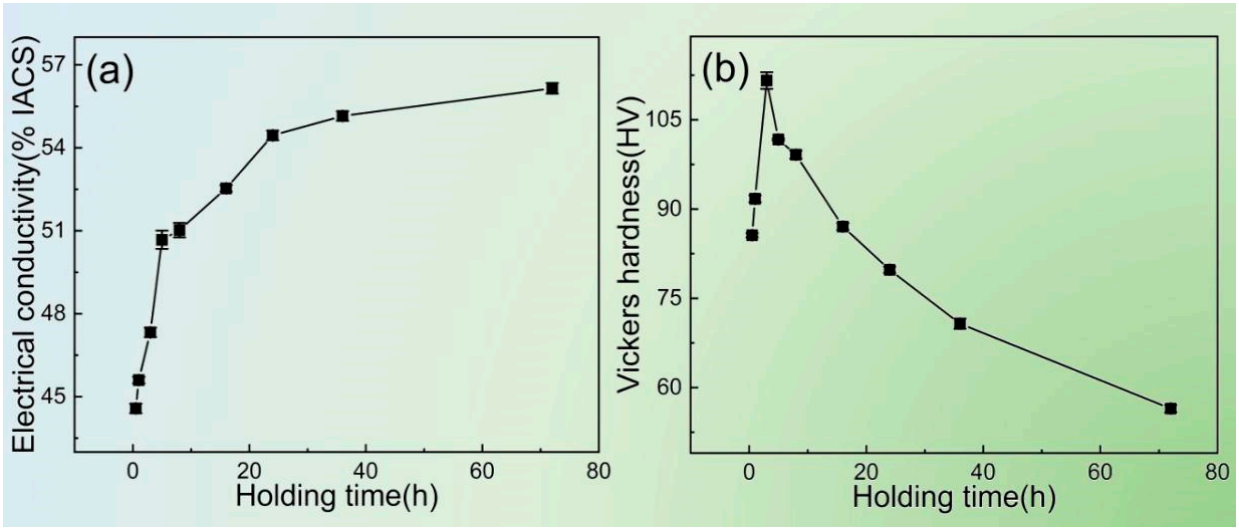


Figure 5. Effect of solution aging heat treatment on EC and hardness of Al-1Si-0.6Mg-0.2Fe alloy: (**a**) change curve of EC, (**b**) change curve of HV.

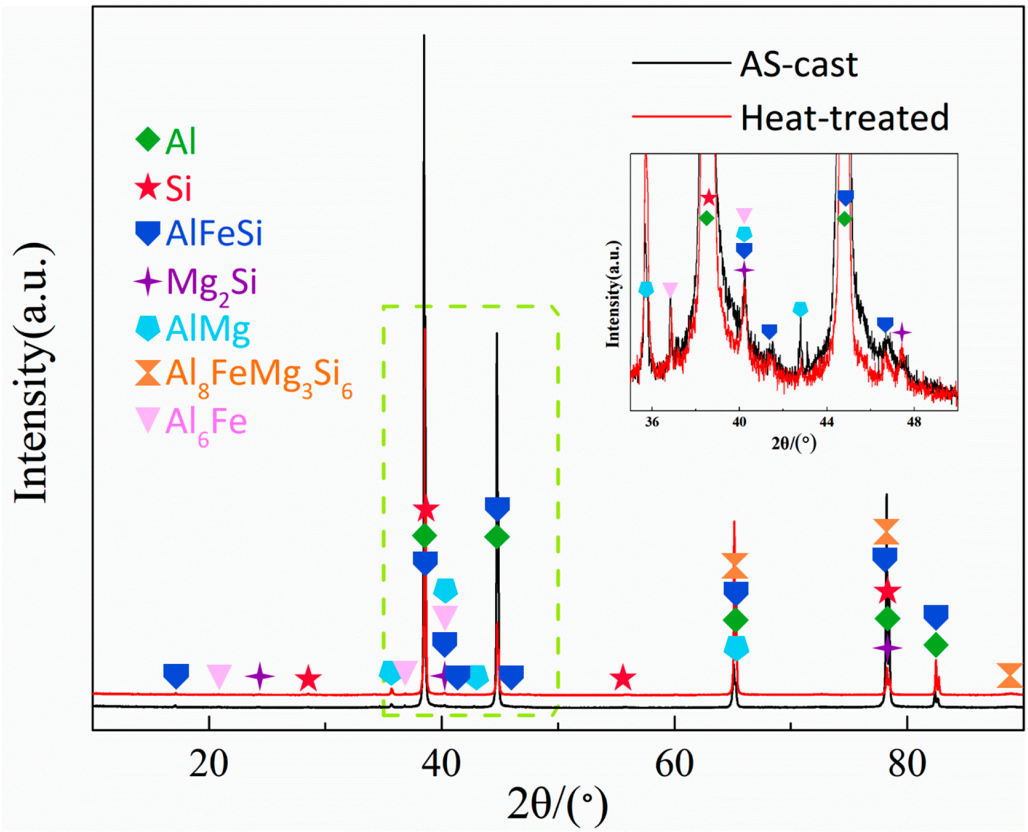


Figure 6. XRD patterns of Al-1Si-0.6Mg-0.2Fe alloys with different states (the heat-treated diffractograms shifted vertically).

Table 2. Analysis results of crystal plane mismatch between AlFeSi phase and Mg_2Si.

	Mismatch Degree (%)		Mismatch Degree (%)
$(\bar{1}01)$ Al_5FeSi ∣ (111) Mg_2Si	0.7	(222) $Al_{0.5}Fe_3Si_{0.5}$ ∣ (400) Mg_2Si	4.0
(111) Al_5FeSi ∣ (200) Mg_2Si	3.0	(400) $Al_{0.5}Fe_3Si_{0.5}$ ∣ (420) Mg_2Si	0.7
(211) Al_5FeSi ∣ (220) Mg_2Si	2.7	(331) $Al_{0.5}Fe_3Si_{0.5}$ ∣ (422) Mg_2Si	1.2
$(\bar{1}22)$ Al_5FeSi ∣ (311) Mg_2Si	3.9	(422) $Al_{0.5}Fe_3Si_{0.5}$ ∣ (511) Mg_2Si	4.5
(112) Al_5FeSi ∣ (222) Mg_2Si	2.4	(422) $Al_{0.5}Fe_3Si_{0.5}$ ∣ (440) Mg_2Si	4.0
(103) Al_5FeSi ∣ (422) Mg_2Si	2.6	(440) $Al_{0.5}Fe_3Si_{0.5}$ ∣ (600) Mg_2Si	4.5
(123) Al_8Fe_2Si ∣ (111) Mg_2Si	0.4	(440) $Al_{0.5}Fe_3Si_{0.5}$ ∣ (620) Mg_2Si	0.7
(125) Al_8Fe_2Si ∣ (200) Mg_2Si	1.1	(440) $Al_{0.5}Fe_3Si_{0.5}$ ∣ (533) Mg_2Si	4.4
(228) Al_8Fe_2Si ∣ (220) Mg_2Si	0.4	(620) $Al_{0.5}Fe_3Si_{0.5}$ ∣ (622) Mg_2Si	5.5
(152) Al_8Fe_2Si ∣ (311) Mg_2Si	0.3	(620) $Al_{0.5}Fe_3Si_{0.5}$ ∣ (444) Mg_2Si	1.3
(154) Al_8Fe_2Si ∣ (222) Mg_2Si	0.9	(620) $Al_{0.5}Fe_3Si_{0.5}$ ∣ (551) Mg_2Si	1.7
(111) $Al_{0.5}Fe_3Si_{0.5}$ ∣ (200) Mg_2Si	4.0		

To further investigate the influence of heat treatment on EC and HV of Al-1Si-0.6Mg-0.2Fe alloy, SEM and EDX are employed to analyze the microstructure before and after heat treatment (as shown in Figure 7). Figure 7a,b show the microstructure change in the Al-1Si-0.6Mg-0.2Fe alloy before and after heat treatment. By comparing, it can be found that, the reinforced particles distributed along grain boundaries in long strips but after T6 heat treatment, the reinforced particles dissolved into the matrix and owing to heat treatment, more Si, Mg and Fe elements precipitated with form of AlFeSi and Mg_2Si, and the reinforced particles diffused to small, short rod like or fine granular. Without heat treatment, many thick pin-striped, short rod-shaped, and granular second phases appear in the alloy. From Figure 7c, it is easy to find that pin-striped AlFeSi is enriched with Mg. In Figure 7d–f, after solution-aging heat treatment, the pin-striped phase size decreases gradually, and the distribution is more uniform. In addition, it is worth emphasizing that pin-striped second phases show a "fracture" phenomenon. Several studies have found that during solidification the phase selection of core–shell structure, which is Fe-containing intermetallic compounds (FIMCs), depends on a non-homogeneous nucleation process [26,27]. The initially nucleated FIMCs will subsequently nucleate binary or ternary eutectic structures [28]. These compounds can be nucleated in eutectic structures such as FIMCs and in other intermetallic phases in aluminum alloys such as Mg_2Si, which readily nucleate on incipient FIMCs [26,27,29]. During heat treatment, from the Al-Fe-Si (Al angle) ternary phase diagram, we know that the AlFeSi phase hardly decomposes at 550 °C. Nevertheless, Si and Mg_2Si phases [26,27], attached to the AlFeSi phase, re-solidify into the Al matrix, disrupting the continuity of coarse pin-striped second phase in the as-cast state. The proper aging temperature and time provide favorable conditions for the diffusion of alloying elements and promote precipitation of solid-solution alloying elements with smaller second phases. From Figure 7d, after heat treatment, the aluminum matrix remains trace amount of Mg and contains little or no Fe, which greatly improves EC. In addition, granular Fe/Mg-rich intermetallic compounds appear after heat treatment, similar to those at Spot 3, which helps to improve the alloy's overall mechanical properties. Finally, the EC and HV of the alloy are optimized simultaneously (as shown in Figure 7e,f).

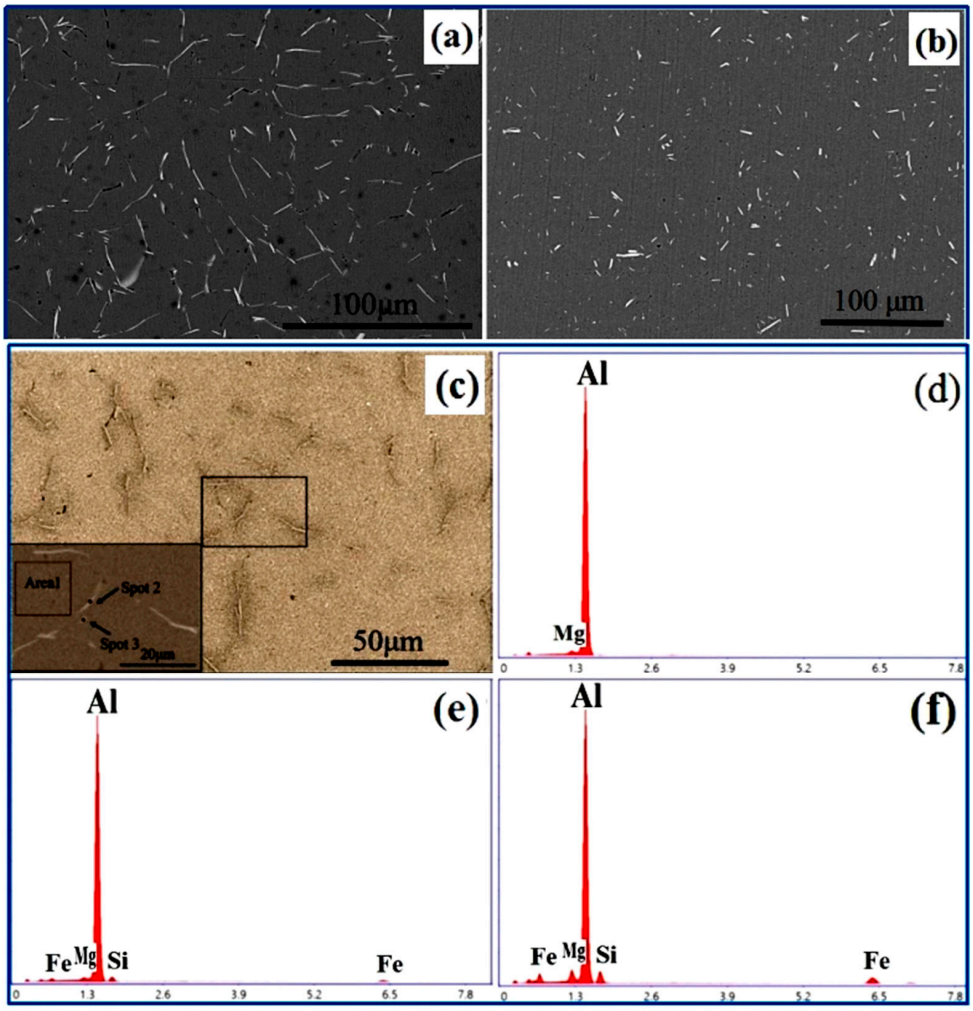


Figure 7. Microstructure and EDX analysis of Al-1Si-0.6Mg-0.2Fe alloy in the as-cast and heat-treated states: (**a**) as-cast, (**b**) as-heat treatment, (**d**–**f**) are EDX analysis of Area1, Spot2, and Spot3 in (**c**), respectively.

3.3. Discussion

Through the analysis about the effect of Mg, Fe alloying treatment on Al-1Si alloy, it is obvious that during the micro-alloying treatment process, the formation of $Al_8FeMg_3Si_6$ interphase plays an important role in the microstructure evolution and HV-EC improvement of Al-1Si alloy. For Al-1Si-0.6Mg-0.2Fe alloy, the content of $Al_8FeMg_3Si_6$ interphase was the most and owing to the formation of $Al_8FeMg_3Si_6$ interphase, the nucleation and growth of AlFeSi and Mg_2Si were influenced. During the heat treatment of Al-1Si-0.6Mg-0.2Fe alloy, more $Al_8FeMg_3Si_6$ interphase can break down into little second phases, such as AlFeSi and Mg_2Si, resulting more Si, Mg and Fe elements precipitated from aluminum matrix. On the one hand, the corresponding aluminum matrix exhibited reduced solute content, and the lattice distortion can be reduced, improving EC of the alloy, on the other hand, forming more micro-/nano- particles was helpful to improve HV of the alloy. In this condition, both of EC and HV can be improved.

After heat treatment, the electrical conductivity (EC) of the Al-1Si-0.6Mg-0.2Fe alloy increases significantly, and the corresponding hardness value (HV) remains relatively high. This phenomenon is depicted in Figure 8, which illustrates the impact mechanism of Mg and Fe alloying treatment and heat treatment on EC and HV. Firstly, owing to Mg and Fe alloying treatment, the existence state of eutectic Si was influenced and more solid solution Si precipitated with form of second phase, such as AlFeSi and Mg_2Si. Owing to Mg and Fe

alloying, the content of Si in solution was reduced and this can reduce lattice distortion of aluminum matrix. Lower lattice distortion is more conducive to efficient electron transport, which is helpful to improve the EC. Furthermore, during T6 heat treatment, more solid solutions consisting of Mg and Si precipitated with form of Mg_2Si and needle-shaped AlFeSi particles fused to grainy particles. And more second phase fused and refined during heat treatment. Smaller second particles have less of an effect on electron scattering, which is helpful to improve electron transport efficiency. So, on one side, electron transport hindered by lattice distortion and second particles was reduced and it is helpful to improve EC, as shown in Figure 8d; on the other side, with proper aging time, the effect of aging reinforcement was strengthened and the corresponding HV can be improved. Consequently, by alloying treatment and proper heat treatment, it is possible to improve EC and HV at the same time. Based on the analysis, a schematic diagram for effect of alloying and heat treatment on microstructure evolution and electron transport efficiency of the Al-1Si alloy was drawn to explain the process in detail. Above all, by Mg and Fe alloying treatment and heat treatment, the microstructure and EC-HV of the Al-1Si alloy can be improved. This process is simple, repeatable and shows good economic benefits for the preparation and processing of conductive aluminum alloy materials.

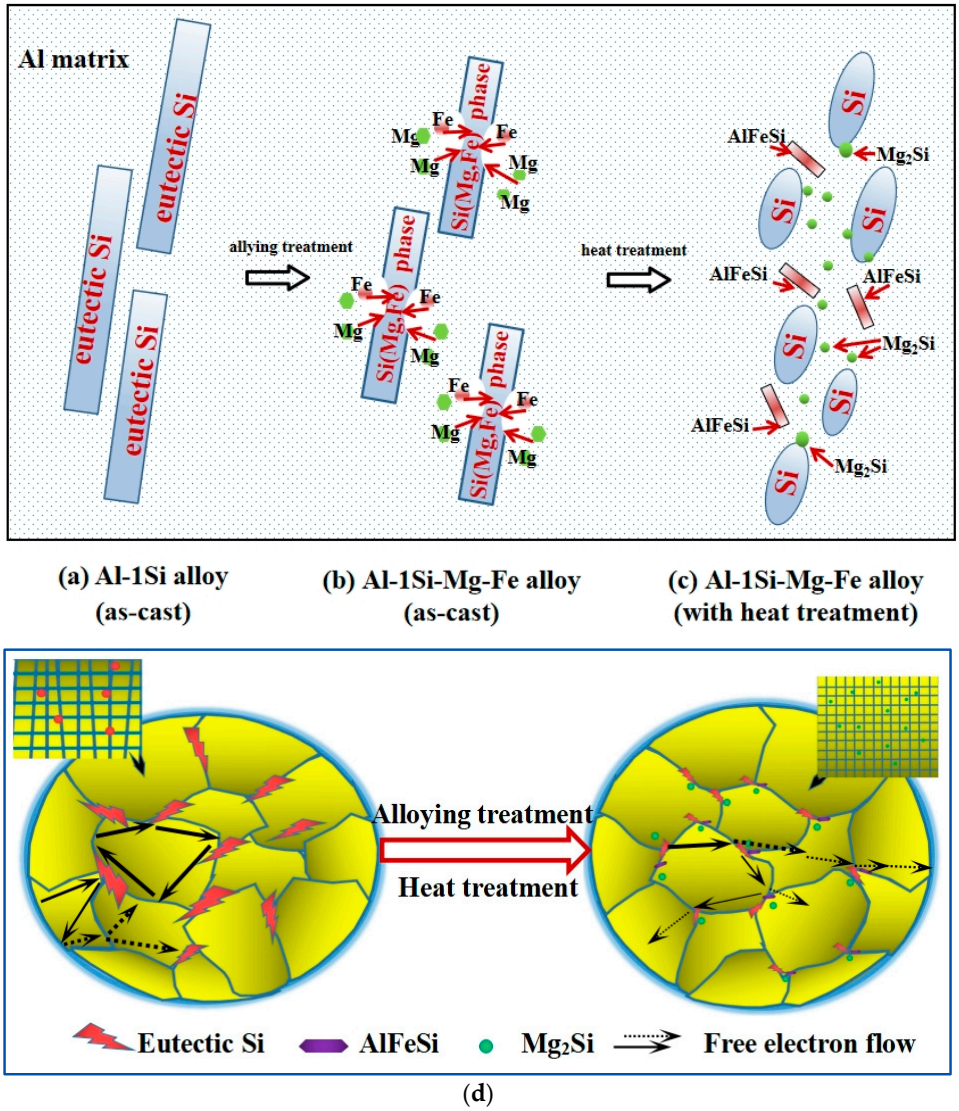


Figure 8. Schematic diagram for effect of Mg and Fe alloying and heat treatment on microstructure evolution (**a**–**c**) and electron transport efficiency (**d**) of Al-1Si-0.6Mg-0.2Fe alloy.

4. Conclusions

In this work, the effect of Mg and Fe addition and heat treatment on electrical conductivity (EC) and hardness value (HV) of Al-1Si is investigated by using a combination of experiments and simulations with JMatPro software. The conclusions are as follows:

1. The optimum contents of Mg and Fe in the Al-1Si alloy are 0.6% and 0.2%, respectively. During the solidification process of the Al-1Si-0.6Mg-0.2Fe alloy, the content of the $Al_8FeMg_3Si_6$ phase is the highest, and in this condition, it can promote more solution Si precipitate with the form of Mg_2Si, and we can control the size and state of Mg_2Si to make it maintain a good lattice match with the aluminum matrix. Furthermore, it is found that $Al_8FeMg_3Si_6$ intermediate product grabbers Fe, resulting in forming slighter AlFeSi, which is helpful to achieve the optimal trade-off between EC and HV.
2. For Al-1Si-0.6Mg-0.2Fe alloy, after 550 °C/2 h + 210 °C/24 h heat treatment, due to Mg_2Si and Si re-solution and recrystallization, part of the FIMCs fused. In this condition, EC and HV reached 54.5% IACS and 79.8 HV, and compared with the Al-1Si alloy, the EC of the Al-1Si-0.6Mg-0.2Fe alloy is increased by 0.2% and the HV is increased by 111.1%, which achieves the optimizing EC and HV.

Author Contributions: Conceptualization: X.C. and H.L.; Methodology: X.C., H.L.; Software: H.L. and C.L.; Validation: Y.W., C.L. and W.S.; Formal analysis: X.C. and C.L.; Investigation: H.L. and Y.W.; Resources: D.T.; Data curation: X.C. and H.L.; Writing—original draft preparation: X.C. and H.L.; Writing—review and editing: X.C.; Project administration: X.C.; Funding acquisition: W.S. and D.T. All authors have read and agreed to the published version of the manuscript.

Funding: Scientific research start-up funds of Guangdong Ocean University (No. YJR24020), Talent promotion plan special fund project of Yangjiang Alloy materials and hardware cutter key industry (No. RCZX2024010), National Key R&D Program of China (2022YFE0126400).

Data Availability Statement: The original contributions presented in the study are included in the article, further inquiries can be directed to the corresponding author.

Conflicts of Interest: The authors declare no conflicts of interest.

References

1. Sauvage, X.; Bobruk, E.V.; Murashkin, M.Y.; Nasedkina, Y.; Enikeev, N.; Valiev, R. Optimization of electrical conductivity and strength combination by structure design at the nanoscale in Al-Mg-Si alloys. *Acta Mater.* **2015**, *98*, 355–366. [CrossRef]
2. Guo, W.; Chen, X.; Liu, P.; Yu, G.; Fu, S.; Fan, J.; Zhou, H.; Liu, H. Effects of Er Additions on the Microstructure, Mechanical Properties, and Electrical Conductivity of the Al-0.4Fe-0.05Si Alloy. *Adv. Eng. Mater.* **2021**, *23*, 2000955. [CrossRef]
3. Ye, H.; Cui, X.; Li, X.; Cui, H.; Zhang, B.; Li, H.; Pan, Y.; Feng, R.; Wu, Y.; Liu, X. Fabrication of hypoeutectic Al-4Si alloy with high electrical conductivity, high plasticity, and medium strength by the dual treatment of Al matrix and eutectic Si microstructure. *J. Alloys Compd.* **2021**, *885*, 161117. [CrossRef]
4. Cui, X.; Ye, H.; Liu, H.; Li, X.; Man, Q.; Li, H.; Cui, H.; Feng, R.; Pan, Y. The improvement mechanism of good matching between electrical conductivity and mechanical properties for Al-4Si-0.8Mg-0.6Fe alloy. *J. Alloys Compd.* **2023**, *938*, 168275. [CrossRef]
5. Karabay, S. Modification of AA-6201 alloy for manufacturing of high conductivity and extra high conductivity wires with property of high tensile stress after artificial aging heat treatment for all-aluminum alloy conductors. *Mater. Des.* **2006**, *27*, 821–832. [CrossRef]
6. Zhao, Q.; Qian, Z.; Cui, X.; Wu, Y.; Liu, X. Optimizing microstructures of dilute Al-Fe-Si alloys designed with enhanced electrical conductivity and tensile strength. *J. Alloys Compd.* **2015**, *650*, 768–776. [CrossRef]
7. Zhao, Q.; Qian, Z.; Cui, X.; Wu, Y.; Liu, X. Influences of Fe, Si, and homogenization on electrical conductivity and mechanical properties of dilute Al-Mg-Si alloy. *J. Alloys Compd.* **2016**, *666*, 50–57. [CrossRef]
8. Kuijpers NC, W.; Kool, W.H.; Koenis, P.T.G.; Nilsen, K.E.; Todd, I.; Van der Zwaag, S. Assessment of different techniques for quantification of α-Al(FeMn)Si and β-AlFeSi intermetallics in AA 6xxx alloys. *Mater. Charact.* **2002**, *49*, 409–420. [CrossRef]
9. Fu, J.; Yang, Z.; Deng, Y.; Wu, Y.F.; Lu, J.Q. Influence of Zr addition on precipitation evolution and performance of Al-Mg-Si alloy conductor. *Mater. Charact.* **2020**, *159*, 110021. [CrossRef]

10. Yuan, W.; Liang, Z. Effect of Zr addition on properties of Al-Mg-Si aluminum alloy used for all aluminum alloy conductor. *Mater. Des.* **2011**, *32*, 4195–4200. [CrossRef]
11. Jing, L.; Cheng, W.; Gan, J. Influencing mechanisms of alloying elements on the electrical conductivity of pure aluminum. *Mater. Rep.* **2021**, *35*, 24101–24106.
12. Luo, K.; Wang, Z.; Meng, L.; Guo, Z. Removal of iron for aluminum recovery from scrap aluminum alloy by supergravity separation with manganese addition. *Chem. Eng. Process. Process Intensif.* **2022**, *173*, 108841. [CrossRef]
13. Chen, H.; Lu, J.; Kong, Y.; Li, K.; Yang, T.; Meingast, A.; Yang, M.; Lu, Q.; Du, Y. Atomic-scale investigation of the crystal structure and interfaces of the β′ precipitate in Al-Mg-Si alloys. *Acta Mater.* **2020**, *185*, 193–203. [CrossRef]
14. Matsuda, K.; Sakaguchi, Y.; Miyata, Y.; Uetani, Y.; Sato, T.; Kamio, A.; Ikeno, S. Precipitation sequence of various kinds of metastable phases in Al-1.0mass% Mg_2Si-0.4mass% Si alloy. *J. Mater. Sci.* **2000**, *35*, 179–189. [CrossRef]
15. Murayama, M.; Hono, K. Pre-precipitate clusters and precipitation processes in Al-Mg-Si alloys. *Acta Mater.* **1999**, *47*, 1537–1548. [CrossRef]
16. Zandbergen, M.W.; Xu, Q.; Cerezo, A.; Smith, G.D. Study of precipitation in Al-Mg-Si alloys by Atom Probe Tomography I. Microstructural changes as a function of aging temperature. *Acta Mater.* **2015**, *101*, 136–148. [CrossRef]
17. Wang, D.; Liang, Y.; Ning, H.; Wang, B. Effects of Zr and Co on the microstructure and mechanical properties of NiAl-based alloys. *J. Alloys Compd.* **2021**, *883*, 160815. [CrossRef]
18. Cheng, Z.; Sun, J.; Cui, J.; Chen, D.; Ren, J.; Wang, T.; Chang, H.; Tai, P.; Zhang, L.; Tian, Y.; et al. Microstructural evolution, strengthening, and high thermal conductivity mechanisms of FeCrV-based medium-entropy alloys with Laves phase precipitation formed by adding minimal Ti. *Mater. Charact.* **2023**, *200*, 112860. [CrossRef]
19. Jiang, H.; Wang, F.; Dong, J. Potential for carbide dispersive precipitation strengthening Ni-based alloy for high temperature. *J. Mater. Res. Technol.* **2023**, *23*, 4860–4865. [CrossRef]
20. Lee, K.; Song, Y.; Kim, S.; Kim, M.; Seol, J.; Cho, K.; Choi, H. Genetic design of new aluminum alloys to overcome strength-ductility trade-off dilemma. *J. Alloys Compd.* **2023**, *947*, 169546. [CrossRef]
21. Liu, J.; Scales, R.J.; Li, B.-S.; Goode, M.; Young, B.A.; Hu, J.; Wilkinson, A.J.; Armstrong, D.E. Controlling microstructure and mechanical properties of Ti-V-Cr-Nb-Ta refractory high entropy alloys through heat treatments. *J. Alloys Compd.* **2023**, *932*, 167651. [CrossRef]
22. Guerra-López, F.V.; Bedolla-Jacuinde, A.; León-Patiño, C.A.; Vázquez-Ramos, M. The effect of small additions of Nb and Ti on the sliding wear behavior of a Co-30Cr-5Mo alloy. *Wear* **2023**, *522*, 204846. [CrossRef]
23. Xu, R.; Wang, W.; Wang, K.; Dai, Q. Finite element simulation of residual stress distribution during selective laser melting of Mg-Y-Sm-Zn-Zr alloy. *Mater. Today Commun.* **2023**, *35*, 105571. [CrossRef]
24. Wei, Y.; Wang, C.; You, J.; Qiu, D.; Gao, Y.; Xu, H.; Xu, J.; Wang, H.-Y. Substantial grain refinement of Al-Mn-Si alloys mediated by collaborative effect of Al-5Ti-1B refiner and sub-rapid solidification. *J. Mater. Sci. Technol.* **2024**, *187*, 230–239. [CrossRef]
25. Fan, W.; Bai, Y.; Zuo, G.; Hao, H. Enhanced grain refinement and mechanical properties of AZ91 alloy by a novel Al-5.1V-2.3B refiner containing VB_2 and VB particles. *Mater. Des.* **2023**, *225*, 111474. [CrossRef]
26. Que, Z.; Mendis, C.L. Formation of θ-$Al_{13}Fe_4$ and the multi-step phase transformations to α-Al_8Fe_2Si, β-Al_5FeSi, and δ-Al_4FeSi_2 in Al-20Si-0.7Fe alloy. *Intermetallics* **2020**, *127*, 106960. [CrossRef]
27. Que, Z.; Mendis, C.L. Heterogeneous nucleation and phase transformation of Fe-rich intermetallic compounds in Al-Mg-Si alloys. *J. Alloys Compd.* **2020**, *836*, 155515. [CrossRef]
28. Que, Z.; Wang, Y.; Fan, Z. Heterogeneous nucleation of eutectic structure in Al-Mg-Si alloys. *Metall. Mater. Trans. A* **2020**, *51*, 2697–2702. [CrossRef]
29. Zhao, Z.; Li, D.; Yan, X.; Chen, Y.; Jia, Z.; Zhang, D.; Han, M.; Wang, X.; Liu, G.; Liu, X.; et al. Insights into the dual effects of Ti on the grain refinement and mechanical properties of hypoeutectic Al-Si alloys. *J. Mater. Sci. Technol.* **2024**, *189*, 44–59. [CrossRef]

Disclaimer/Publisher's Note: The statements, opinions and data contained in all publications are solely those of the individual author(s) and contributor(s) and not of MDPI and/or the editor(s). MDPI and/or the editor(s) disclaim responsibility for any injury to people or property resulting from any ideas, methods, instructions or products referred to in the content.